Dynamics in spinor condensates tuned by a microwave dressing field

L. Zhao, J. Jiang, T. Tang, M. Webb, and Y. Liu*

Department of Physics, Oklahoma State University, Stillwater, Oklahoma 74078, USA

(Received 24 October 2013; revised manuscript received 16 December 2013; published 10 February 2014)

We experimentally study spin dynamics in a sodium antiferromagnetic spinor condensate as a result of spin-dependent interactions c and microwave dressing field interactions characterized by the net quadratic Zeeman effect $q_{\rm net}$. In contrast to magnetic fields, microwave dressing fields enable us to access both negative and positive values of $q_{\rm net}$. We find an experimental signature to determine the sign of $q_{\rm net}$ and observe harmonic spin population oscillations at every $q_{\rm net}$ except near each separatrix in phase space where spin oscillation period diverges. No spin domains and spatial modes are observed in our system. Our data in the negative $q_{\rm net}$ region exactly resembles what is predicted to occur in a ferromagnetic spinor condensate in the positive $q_{\rm net}$ region. This observation agrees with an important prediction derived from the mean-field theory: spin dynamics in spin-1 condensates substantially depends on the sign of $q_{\rm net}/c$. This work uses only one atomic species to reveal mean-field spin dynamics, especially the remarkably different relationship between each separatrix and the magnetization, of spin-1 antiferromagnetic and ferromagnetic spinor condensates.

DOI: 10.1103/PhysRevA.89.023608 PACS number(s): 67.85.Hj, 32.60.+i, 03.75.Kk, 03.75.Mn

I. INTRODUCTION

An atomic Bose-Einstein condensate (BEC) is a state where all atoms have a single collective wave function for their spatial degrees of freedom. The key benefit of spinor BECs is the additional spin degree of freedom. Together with Feshbach resonances and optical lattices which tune the interatomic interactions, spinor BECs constitute a fascinating collective quantum system offering an unprecedented degree of control over such parameters as spin, temperature, and the dimensionality of the system [1,2]. Spinor BECs have become one of the fastest-moving research frontiers in the past 15 years. A number of atomic species have proven to be perfect candidates in the study of spinor BECs, such as $F = 1$ and $F = 2$ hyperfine spin states of ^{87}Rb atoms [1–7] and $F = 1$ hyperfine spin manifolds of ^{23}Na atoms [8–12]. Many interesting phenomena due to the interconversion among multiple spin states and magnetic field interactions have been experimentally demonstrated in spinor BECs, such as spin population dynamics [1–9], quantum number fluctuation [10,13], various quantum phase transitions [1,9,11,12], and quantum spin-nematic squeezing [14]. Spinor BEC systems have been successfully described with a classical two-dimensional phase space [1,2,15–17], a rotor model [18], or a quantum model [13,17].

In this paper, we experimentally study spin-mixing dynamics in a $F = 1$ sodium spinor condensate starting from a nonequilibrium initial state, driven by the net quadratic Zeeman energy $q_{\rm net} = q_M + q_B$ and antiferromagnetic spin-dependent interactions c. Here q_B and q_M are the quadratic Zeeman shifts induced by magnetic fields and microwave dressing fields, respectively. The spin-dependent interaction energy c is proportional to the mean BEC density and the difference in the $f = 0$ and $f = 2$ s-wave scattering lengths, where f is the summed spin angular momentum in a collision. It is well known that $c > 0$ (or $c < 0$) in $F = 1$ antiferromagnetic ^{23}Na (or ferromagnetic ^{87}Rb) spinor BECs. In contrast to a magnetic field, a microwave dressing field enables us to access both negative and positive values of $q_{\rm net}$. A method to characterize microwave dressing fields and an approach to adiabatically sweep $q_{\rm net}$ from $-\infty$ to $+\infty$ are also explained. In both negative and positive $q_{\rm net}$ regions, we observe spin population oscillations resulting from coherent collisional interconversion among two $|F = 1, m_F = 0\rangle$ atoms, one $|F = 1, m_F = +1\rangle$ atom, and one $|F = 1, m_F = -1\rangle$ atom. In every spin oscillation studied in this paper, our data show that the population of the $m_F = 0$ state averaged over time is always larger (or smaller) than its initial value as long as $q_{\rm net} < 0$ (or $q_{\rm net} > 0$). This observation provides a clear experimental signature to determine the sign of $q_{\rm net}$. We also find a remarkably different relationship between the total magnetization m and a separatrix in phase space where spin oscillation period diverges: The position of the separatrix moves slightly with m in the positive $q_{\rm net}$ region, while the separatrix quickly disappears when m is away from zero in the negative $q_{\rm net}$ region. Our data agree with an important prediction derived by Ref. [17]: The spin-mixing dynamics in $F = 1$ spinor condensates substantially depends on the sign of $R = q_{\rm net}/c$. This work uses only one atomic species to reveal mean-field spin dynamics, especially the relationship between each separatrix and the magnetization, which are predicted to appear differently in $F = 1$ antiferromagnetic and ferromagnetic spinor condensates.

Because no spin domains and spatial modes are observed in our system, the single spatial mode approximation (SMA), in which all spin states have the same spatial wave function, appears to be a proper theoretical model to understand our data. Similarly to Refs. [1,16], we take into account the conservation of the total atom number and the total magnetization m. Spin-mixing dynamics in a $F = 1$ spinor BEC can thus be described with a two-dimensional (ρ_0 versus θ) phase space, where the fractional population ρ_{m_F} and the phase θ_{m_F} of each m_F state are independent of position. The BEC energy E and the time evolution of ρ_0 and θ may be expressed as [1,16]

$$\begin{aligned} E &= q_{\rm net}(1-\rho_0) \\ &\quad + c\rho_0[(1-\rho_0) + \sqrt{(1-\rho_0)^2 - m^2}\cos\theta], \\ \dot{\rho}_0 &= -(2/\hbar)\partial E/\partial\theta, \dot{\theta} = (2/\hbar)\partial E/\partial\rho_0. \end{aligned} \tag{1}$$

*yingmei.liu@okstate.edu

Here $\theta = \theta_{+1} + \theta_{-1} - 2\theta_0$ is the relative phase among the three m_F spin states and $\hbar$ is the reduced Planck constant. The induced linear Zeeman shift remains the same during the collisional spin interconversion and is thus ignored. The total magnetization is $m = \rho_{+1} - \rho_{-1}$. Spin dynamics in $F = 1$ antiferromagnetic and ferromagnetic spinor BECs have been studied in magnetic fields where $q_{\rm net} = q_B \propto B^2 > 0$ with ^{23}Na and ^{87}Rb atoms, respectively [1]. A few methods have been explored for generating a negative quadratic Zeeman shift, such as via a microwave dressing field [1,11,19–21] or through a linearly polarized off-resonant laser beam [22]. In this paper, we choose the first method.

II. EXPERIMENTAL SETUP

The experimental setup is similar to that illustrated in our previous work [23]. Hot ^{23}Na atoms are slowed by a spin-flip Zeeman slower, captured in a standard magneto-optical trap, cooled through a polarization gradient cooling process to 40 μK, and loaded into a crossed optical dipole trap originating from a linearly polarized high-power infrared laser at 1064 nm. After an optimized 6-s forced evaporative cooling process, a pure $F = 1$ BEC of 1.0×10^5 sodium atoms is created. The spin healing length and the Thomas-Fermi radii of a typical condensate studied in this paper are 13 μm and (6.1, 6.1, 4.3) μm, respectively. We can polarize atoms in the $F = 1$ BEC fully to the $|F = 1, m_F = -1\rangle$ state by applying a weak magnetic field gradient during the first half of the forced evaporation (or fully to the $|F = 1, m_F = 0\rangle$ state by adding a very strong magnetic bias field during the entire 6-s forced evaporation). We then ramp up a small magnetic bias field with its strength B being 271.5(4) mG, while turning off the field gradient. An rf-pulse resonant with the linear Zeeman splitting is applied to prepare an initial state with any desired combination of the three m_F states, which is followed by abruptly switching on an off-resonant microwave pulse to generate a proper microwave dressing field. To create sufficiently large $q_{\rm net}$, a microwave antenna designed for a frequency near the $|F = 1\rangle \leftrightarrow |F = 2\rangle$ transition is placed a few inches above the center of the magneto-optical trap and connected to a function generator outputting a maximum power of 10 W. The actual power used in this paper is $\sim$8 W. After various hold times t in the optical dipole trap, the microwave dressing fields are quickly turned off. Populations of the multiple spin states are then measured via the standard absorption imaging preceded by a 3-ms Stern-Gerlach separation and a 7-ms time of flight.

The exact value of $q_{\rm net}$ is carefully calibrated from a few experimental parameters, such as the polarization and frequency of a microwave pulse. Similarly to Refs. [19,21], we express the value of $q_{\rm net}$ as

$$\begin{aligned} q_{\rm net} &= q_{\rm B} + q_{\rm M} \\ &= aB^2h + \frac{\delta E|_{m_F=1} + \delta E|_{m_F=-1} - 2\delta E|_{m_F=0}}{2}, \\ \delta E|_{m_F} &= \frac{h}{4}\sum_{k=0,\pm1} \frac{\Omega^2_{m_F,m_F+k}}{\Delta_{m_F,m_F+k}} \\ &= \frac{h}{4}\sum_{k=0,\pm1} \frac{\Omega^2_{m_F,m_F+k}}{\Delta - [(m_F+k)/2 - (-m_F/2)]\mu_B B}, \end{aligned} \quad (2)$$

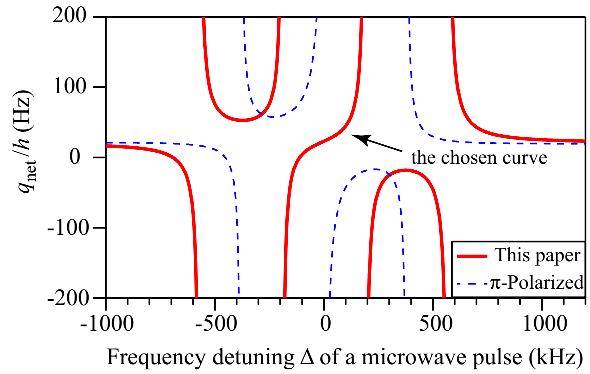

FIG. 1. (Color online) $q_{\rm net}$ as a function of Δ. The residual magnetic field is $B = 271.5(4)$ mG. Dashed blue lines represent the predictions derived from Eq. (2) when the microwave pulse is purely π polarized and its corresponding on-resonance Rabi frequencies are $\Omega_{-1,-2} = \Omega_{0,-1} = \Omega_{1,0} = \Omega_{-1,0} = \Omega_{0,1} = \Omega_{1,2} = 0$, $\Omega_{-1,-1} = \Omega_{1,1} = 4.2$ kHz, and $\Omega_{0,0} = 4.9$ kHz. Solid red lines represent the predictions from Eq. (2) for a typical microwave pulse used in this paper. The specially chosen polarization of this pulse yields nine on-resonance Rabi frequencies as follows: $\Omega_{-1,-2} = 5.1$ kHz, $\Omega_{0,-1} = 3.6$ kHz, and $\Omega_{1,0} = 2.1$ kHz are from the σ^--polarized component of the pulse; $\Omega_{-1,-1} = \Omega_{0,0} = \Omega_{1,1} = 0$ are from the π-polarized component of the pulse; and $\Omega_{-1,0} = 2.3$ kHz, $\Omega_{0,1} = 3.9$ kHz, and $\Omega_{1,2} = 5.5$ kHz are from the σ^+-polarized component of the pulse (see text). In this paper, Δ is tuned within the range of -190 kHz to 190 kHz from the $|F = 1, m_F = 0\rangle \leftrightarrow |F = 2, m_F = 0\rangle$ transition.

where $a \approx 277$ Hz/G^2 (or $a \approx 71$ Hz/G^2) for $F = 1$ ^{23}Na (or ^{87}Rb) atoms, the microwave pulse is detuned by Δ from the $|F = 1, m_F = 0\rangle \leftrightarrow |F = 2, m_F = 0\rangle$ transition, and h is the Planck constant. We define k as 0 or ±1 for a π- or a $\sigma^\pm$-polarized microwave pulse, respectively. For a given polarization k, the allowed transition is $|F = 1, m_F\rangle \leftrightarrow |F = 2, m_F + k\rangle$ and its on-resonance Rabi frequency is $\Omega_{m_F,m_F+k} \propto \sqrt{I_k} C_{m_F,m_F+k}$, where C_{m_F,m_F+k} is the Clebsch-Gordan coefficient of the transition and I_k is the intensity of this purely polarized microwave pulse. We also define $\Delta_{m_F,m_F+k} = \Delta - [(m_F+k)/2 - (-m_F/2)]\mu_B B$ as the frequency detuning of the microwave pulse with respect to the $|F = 1, m_F\rangle \rightarrow |F = 2, m_F + k\rangle$ transition, where μ_B is the Bohr magneton.

A purely π-polarized microwave pulse has been a popular choice in some publications [1,20,21]. However, we apply microwave pulses of a specially chosen polarization, in order to continuously scan $q_{\rm net}$ from large negative values to big positive values at a moderate microwave power. Figure 1 compares microwave dressing fields induced by a typical microwave pulse used in this paper and a purely π-polarized microwave pulse. This comparison clearly shows that it is possible to continuously or adiabatically sweep $q_{\rm net}$ from $-\infty$ to $+\infty$ simply by continuously tuning Δ from -190 kHz to 190 kHz with our specially chosen microwave pulses at a power of 8 W. Another advantage of choosing such microwave pulses is to conveniently place the microwave antenna on our apparatus without blocking optical components. To ensure an accurate calibration of $q_{\rm net}$ based on Eq. (2), we measure the nine on-resonance Rabi frequencies Ω daily through monitoring the number of atoms excited by a resonant microwave pulse

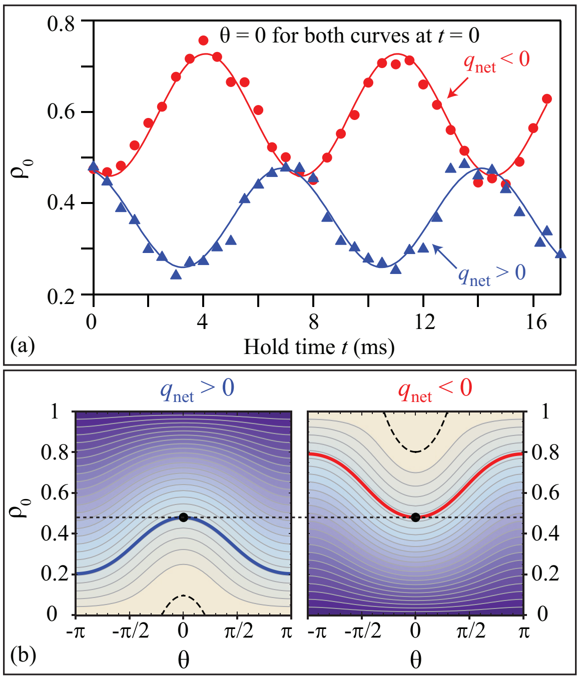

FIG. 2. (Color online) (a) Time evolutions of ρ_0 at $q_{net}/h = +93\text{Hz} > 0$ (solid blue triangles) and $q_{net}/h = -83$ Hz < 0 (solid red circles) with $m = 0$ and $c/h = 52(1)$ Hz. It is important to note that the two curves start from the same initial state with $\theta|_{t=0} = 0$. Solid lines are sinusoidal fits to the data. (b) Equal-energy contour plots based on Eq. (1) for the two experimental conditions shown in Fig. 2(a), i.e., $q_{net} > 0$ (left) and $q_{net} < 0$ (right). The heavy solid blue and red lines represent the energy of the above two experimental conditions, respectively. The dotted black horizontal line is to emphasize the fact that the above two experiments start with the same initial state which is marked by the solid black circles. Dashed black lines represent the energy of the separatrix between the running and oscillatory phase solutions. Darker colors correspond to lower energies.

to the $F = 2$ state as a function of the pulse duration. A typical example of the Rabi frequency measurement is shown in Fig. 3(a). We find that uncertainties of Ω and q_{net} are $\sim$2% and $\sim$5%, respectively.

III. DYNAMICS OF SPINOR CONDENSATES IN MICROWAVE DRESSING FIELDS

We observe spin oscillations at every given value of q_{net} within a wide range, i.e., -240 Hz $\leqslant q_{net}/h \leqslant 240$ Hz. Typical time evolutions of ρ_0 starting with the same nonequilibrium initial state at a negative and a positive q_{net} are shown in Fig. 2(a). We find that these evolutions can be well fit by sinusoidal functions of the similar oscillation period T and amplitude A. Note that the hold time t is kept between zero and $2T < 100$ ms, in order to ensure accurate measurements of spin dynamics and avoid significant atom losses due to the presence of off-resonant microwave pulses. On the other hand, our data in Fig. 2(a) show that the value of $\langle\rho_0\rangle$ drastically differs in the two spin oscillations: $\langle\rho_0\rangle > \rho_0|_{t=0}$ as long as $q_{net} < 0$, while $\langle\rho_0\rangle < \rho_0|_{t=0}$ if $q_{net} > 0$. Here $\langle\rho_0\rangle$ is the average value of ρ_0 over time in a spin oscillation and $\rho_0|_{t=0}$ is the initial value of ρ_0. This phenomenon is observed at every value of q_{net} when spin oscillations start with the same initial state, although the period T and amplitude A change with q_{net}. The above observations agree well with predictions from the mean-field SMA theory [i.e., Eq. (1)] as shown by the heavy solid lines in Fig. 2(b): ρ_0 is limited between $(\rho_0|_{t=0} - 2A)$ and $\rho_0|_{t=0}$ at $q_{net} > 0$, while it is restricted between $\rho_0|_{t=0}$ and $(\rho_0|_{t=0} + 2A)$ at $q_{net} < 0$. We can thus use the phenomenon to conveniently determine the sign of q_{net}, i.e., by comparing the value of $\langle\rho_0\rangle$ of a spin oscillation to the value of $\rho_0|_{t=0}$.

The value of T as a function of q_{net} is then plotted in Fig. 3 for $m = 0$ and $m = 0.2$, which demonstrates two interesting results. First, when $m = 0$, the spin oscillation is harmonic except near the critical values (i.e., $q_{net}/h = \pm 52$ Hz) where the period diverges. This agrees with the predictions derived from Eq. (1), as shown by the dotted red line in Fig. 3. The energy contour E_{sep} where the oscillation becomes anharmonic is defined as a separatrix in phase space. A point on the separatrix satisfies the equation $\dot{\rho}_0 = \dot{\theta} = 0$ according to the mean-field SMA theory. In fact, for our sodium system with $c > 0$, $E_{sep} = q_{net}$ for $q_{net} > 0$, while $E_{sep} = 0$ at $m = 0$ for $q_{net} < 0$. Figure 3 shows that the T versus q_{net} curve is symmetric with respect to the $q_{net} = 0$ axis at $m = 0$. The period T decreases rapidly with increasing $|q_{net}|$ when $|q_{net}|$ is large, which corresponds to the “Zeeman regime” with running phase solutions. In the opposite limit, the period only weakly depends on $|q_{net}|$, which represents the “interaction regime” with oscillatory phase solutions. Here $|q_{net}|$ is the absolute value of q_{net}. The value of θ is (or is not) restricted in the regions with oscillatory (or running) phase solutions. References [8,9] reported observations of the similar phenomena for $q_{net} > 0$ with a $F = 1$ antiferromagnetic spinor condensate; however, they did not access the negative q_{net} region.

Figure 3 also demonstrates a remarkably different relationship between the total magnetization m and the separatrix in phase space: the position of the separatrix moves slightly with m in the positive q_{net} region, while the separatrix quickly disappears when m is away from zero in the negative q_{net} region. Good agreements between our data and the mean-field SMA theory are shown in the inset [Fig. 3(b)] and the main figure in Fig. 3. Interestingly, we find that the spin dynamics which appear in our antiferromagnetic sodium system in the negative q_{net} region exactly resembles what is predicted to occur in a ferromagnetic spinor condensate in the positive q_{net} region [16,17]. Note that $R = q_{net}/c$ is negative in both of these two cases. This observation agrees with an important prediction made by Ref. [17]: The spin-mixing dynamics in $F = 1$ spinor condensates substantially depends on the sign of R. As a matter of fact, our results in the negative q_{net} region are similar to those reported with a $F = 1$ ferromagnetic ^{87}Rb spinor condensate in magnetic fields where $q_{net} > 0$ [1,3]. It is worth noting that our data in Fig. 3 may also be extrapolated to understand the relationship between the separatrix and m in the ferromagnetic Rb system, although this relationship has not been experimentally explored yet. This paper may thus be the first to use only one atomic species to reveal mean-field spin dynamics, especially the different relationship between each separatrix and the magnetization of $F = 1$ antiferromagnetic and ferromagnetic spinor condensates.

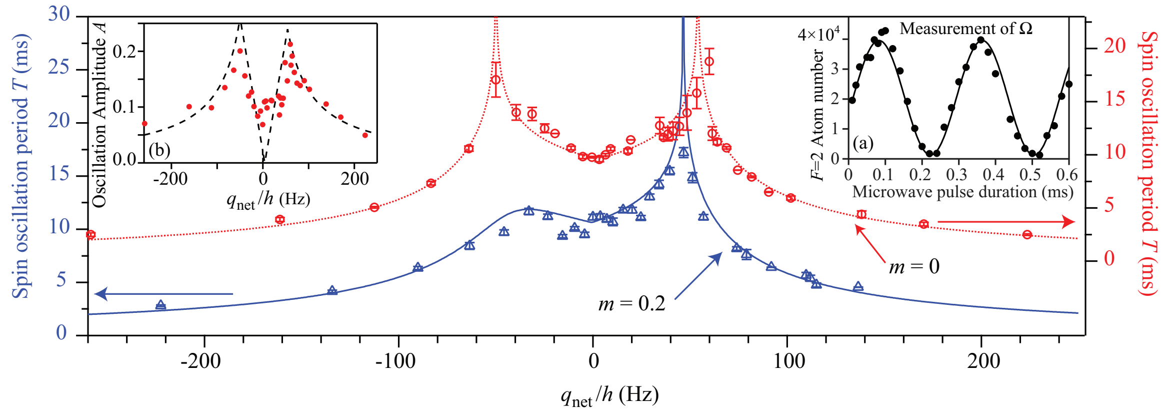

FIG. 3. (Color online) The spin oscillation period as a function of q_{net} for $m = 0$ (open red circles) and $m = 0.2$ (open blue triangles). The lines are fits based on Eq. (1), which yield the following fit parameters: $\rho_0|_{t=0} = 0.48$, $\theta|_{t=0} = 0$, and $c/h = 52(1)$ Hz for $m = 0$ and $\rho_0|_{t=0} = 0.48$, $\theta|_{t=0} = 0$, and $c/h = 47(1)$ Hz for $m = 0.2$. The fit parameters are within the 5% uncertainty of our measurements. Note the different scales of the left and right vertical axes. Inset (a): The number of $F = 2$ atoms excited by a resonant microwave pulse as a function of the pulse duration. The solid line is a sinusoidal fit to extract the on-resonance Rabi frequency Ω of the pulse. Inset (b): Amplitudes A of spin oscillations shown in the main figure as a function of q_{net} at $m = 0$. The dashed black line is a fit based on Eq. (1) with the same set of fit parameters as that applied in the main figure.

IV. CONCLUSION

In conclusion, we have experimentally studied spin dynamics of a sodium spinor condensate in a microwave dressing field. In both negative and positive q_{net} regions, we have observed harmonic spin oscillations and found that the sign of q_{net} can be determined by comparing $\langle\rho_0\rangle$ to $\rho_0|_{t=0}$. Our data also demonstrate that the position of the separatrix in phase space moves slightly with m in the positive q_{net} region, while the separatrix quickly disappears when m is away from zero in the negative q_{net} region. Our data can be well fit by the mean-field theory and agree with one of its important predictions: The spin-mixing dynamics in $F = 1$ spinor condensates substantially depends on the sign of $R = q_{\text{net}}/c$. This work uses only one atomic species to reveal mean-field spin dynamics and the different dependence of each separatrix on m in $F = 1$ antiferromagnetic and ferromagnetic spinor condensates. In addition, microwave pulses used in this paper can be applied to cancel out stray magnetic fields and adiabatically sweep q_{net} from $-\infty$ to $+\infty$. This allows studies on interesting but unexplored phenomena at $q_{\text{net}} = 0$, for example, realizing a maximally entangled Dicke state with antiferromagnetic spinor condensates through quantum phase transitions [24].

ACKNOWLEDGMENTS

We thank the Army Research Office, Oklahoma Center for the Advancement of Science and Technology, and Oak Ridge Associated Universities for financial support. M.W. thanks the Niblack Research Scholar program.

[1] D. M. Stamper-Kurn and M. Ueda, Rev. Mod. Phys. **85**, 1191 (2013).

[2] Y. Kawaguchi and M. Ueda, Phys. Rep. **520**, 253 (2012).

[3] M.-S. Chang, Q. Qin, W. Zhang, L. You, and M. S. Chapman, Nat. Phys. **1**, 111 (2005).

[4] A. Widera, F. Gerbier, S. Fölling, T. Gericke, O. Mandel, and I. Bloch, New J. Phys. **8**, 152 (2006).

[5] J. Kronjäger, C. Becker, P. Navez, K. Bongs, and K. Sengstock, Phys. Rev. Lett. **97**, 110404 (2006).

[6] H. Schmaljohann, M. Erhard, J. Kronjäger, M. Kottke, S. van Staa, L. Cacciapuoti, J. J. Arlt, K. Bongs, and K. Sengstock, Phys. Rev. Lett. **92**, 040402 (2004).

[7] T. Kuwamoto, K. Araki, T. Eno, and T. Hirano, Phys. Rev. A **69**, 063604 (2004).

[8] A. T. Black, E. Gomez, L. D. Turner, S. Jung, and P. D. Lett, Phys. Rev. Lett. **99**, 070403 (2007).

[9] Y. Liu, S. Jung, S. E. Maxwell, L. D. Turner, E. Tiesinga, and P. D. Lett, Phys. Rev. Lett. **102**, 125301 (2009).

[10] Y. Liu, E. Gomez, S. E. Maxwell, L. D. Turner, E. Tiesinga, and P. D. Lett, Phys. Rev. Lett. **102**, 225301 (2009).

[11] E. M. Bookjans, A. Vinit, and C. Raman, Phys. Rev. Lett. **107**, 195306 (2011).

[12] D. Jacob, L. Shao, V. Corre, T. Zibold, L. De Sarlo, E. Mimoun, J. Dalibard, and F. Gerbier, Phys. Rev. A **86**, 061601 (2012).

[13] L. Chang, Q. Zhai, R. Lu, and L. You, Phys. Rev. Lett. **99**, 080402 (2007).

[14] C. D. Hamley, C. S. Gerving, T. M. Hoang, E. M. Bookjans, and M. S. Chapman, Nature Physics **8**, 305 (2012).

[15] W. Zhang, S. Yi, and L. You, New J. Phys. **5**, 77 (2003).

[16] W. Zhang, D. L. Zhou, M.-S. Chang, M. S. Chapman, and L. You, Phys. Rev. A **72**, 013602 (2005).

[17] A. Lamacraft, Phys. Rev. A **83**, 033605 (2011).

[18] R. Barnett, J. D. Sau, and S. Das Sarma, Phys. Rev. A **82**, 031602 (2010).

[19] F. Gerbier, A. Widera, S. Fölling, O. Mandel, and I. Bloch, Phys. Rev. A **73**, 041602(R) (2006).
[20] S. R. Leslie, J. Guzman, M. Vengalattore, J. D. Sau, M. L. Cohen, and D. M. Stamper-Kurn, Phys. Rev. A **79**, 043631 (2009).
[21] Sabrina R. A. Leslie, Ph.D. thesis, University of California, Berkeley, 2008.
[22] L. Santos, M. Fattori, J. Stuhler, and T. Pfau, Phys. Rev. A **75**, 053606 (2007).
[23] J. Jiang, L. Zhao, M. Webb, N. Jiang, H. Yang, and Y. Liu, Phys. Rev. A **88**, 033620 (2013).
[24] Z. Zhang and L.-M. Duan, Phys. Rev. Lett. **111**, 180401 (2013).